John von Neumann Institute for Computing


# The Transverse Spin Structure of the Nucleon

G. Schierholz

published in

*NIC Symposium 2008*,
G. Münster, D. Wolf, M. Kremer (Editors),
John von Neumann Institute for Computing, Jülich,
NIC Series, Vol. **39**, ISBN 978-3-9810843-5-1, pp. 135-142, 2008.



http://www.fz-juelich.de/nic-series/volume39

# The Transverse Spin Structure of the Nucleon

**G. Schierholz**

Deutsches Elektronen-Synchrotron DESY
*E-mail: Gerrit.Schierholz@desy.de*

– For the *QCDSF Collaboration* –

Recent advances in algorithms and computer technology have enabled lattice QCD to make increasingly quantitative calculations of hadron structure. In this contribution we shall present first results on the transverse spin structure of nucleon and pion from simulations of $N_f = 2$ flavours of light dynamical sea quarks.

## 1 Introduction

A major scientific goal of elementary particle physics is to achieve a quantitative understanding of the structure and interactions of hadrons in terms of their quark and gluon constituents. Although a quarter of a century has passed since the experimental discovery of quarks in the nucleon and the invention of QCD, understanding how QCD works remains one of the great puzzles in physics.

Generalized Parton Distributions (GPDs)[1,2] are the modern tool to deliver a detailed description of the microscopic structure of hadrons. They allow to map out the longitudinal and transverse distributions of quarks and gluons in the fast moving hadron, thus providing an essentially holographic picture of mesons and baryons. This is illustrated in Fig. 1,

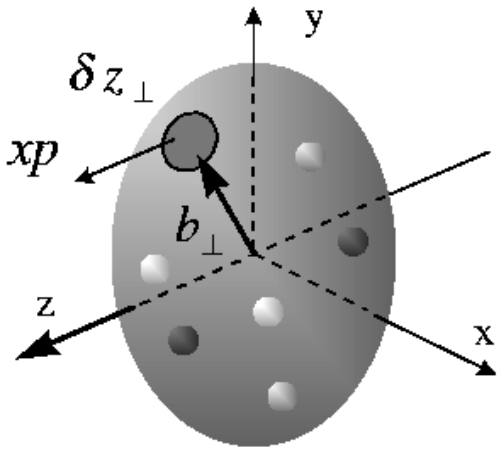


Figure 1. Pictorial view of the nucleon moving with momentum $p$ in the $z$-direction in terms of its quark constituents.

where we show

$$\rho^q(x, b_\perp) = H^q(x, b_\perp^2)\,, \tag{1}$$

which describes the probability of finding an unpolarized quark of type $q$ with fractional longitudinal momentum $x$ at impact parameter $b_\perp$ in the unpolarized nucleon. The impact parameter $b_\perp$ denotes the distance between the quark and the centre of momentum of the nucleon in the plane perpendicular to its momentum. In different kinematic limits of the GPDs one recovers the familiar elastic form factors, parton densities and distribution amplitudes. For example,

$$q(x) = \int \frac{d^2 b_\perp}{(2\pi)^2} H^q(x, b_\perp^2)\,, \tag{2}$$

where $q(x)$ is the ordinary quark parton distribution of the nucleon. GPDs are directly relevant to present and future experiments at CERN, DESY, GSI, JLab, MAMI and RHIC-spin.

Recent advances in lattice field theory, numerical algorithms and computer technology have enabled us to compute GPDs from first principles. In this contribution I shall report first results on the spin structure of nucleon and pion.

## 2 Spin Structure of the Nucleon

Let us consider a fast moving nucleon[a] with transverse spin $S_\perp$ (with respect to the nucleon's momentum)[3]. We are interested in the density of quarks $\rho^q(x, b_\perp, s_\perp, S_\perp)$, $q = u$ and $d$, with fractional momentum $x$ and transverse spin $s_\perp$. In lattice calculations only moments of $\rho(x, b_\perp, s_\perp, S_\perp)$ are accessible[4]:

$$\begin{aligned}\rho^{q\,n}(b_\perp, s_\perp, S_\perp) = \int_{-1}^{1} dx\, x^{n-1} \rho^q(x, b_\perp, s_\perp, S_\perp) = \frac{1}{2}\Big\{ A_n^q(b_\perp^2) + s_\perp^i S_\perp^i \Big( A_{Tn}^q(b_\perp^2) \\ - \frac{1}{4m_N^2} \Delta_{b_\perp} \widetilde{A}_{Tn}^q(b_\perp^2) \Big) + \frac{b_\perp^j \epsilon^{ji}}{m_N} \Big( S_\perp^i B_n^{q\,\prime}(b_\perp^2) + s_\perp^i \overline{B}_{Tn}^{q\,\prime}(b_\perp^2) \Big) \\ + s_\perp^i (2 b_\perp^i b_\perp^j - b_\perp^2 \delta^{ij}) S_\perp^j \frac{1}{m_N^2} \widetilde{A}_{Tn}^{q\,\prime\prime}(b_\perp^2) \Big\}\,,\end{aligned} \tag{3}$$

where $m_N$ is the nucleon mass and $A_n$, $A_{Tn}$, $\widetilde{A}_{Tn}$, $B_n$ and $B_{Tn}$ are generalized form factors (GFFs). The momentum space GFFs are obtained from off-forward nucleon matrix elements of composite operators. For example,

$$\begin{aligned}\langle p', S' |\, \mathcal{O}_T^{q\,\mu\nu}\, | p, S \rangle = \overline{u}(p', S') \Big\{ \sigma^{\mu\nu} \gamma_5 \big( A_{T1}^q(t) - \frac{t}{2m_N^2} \widetilde{A}_{T1}^q(t) \big) \\ + \frac{\epsilon^{\mu\nu\alpha\beta} \Delta_\alpha \gamma_\beta}{2m_N} \overline{B}_{T1}^q(t) - \frac{\Delta^{[\mu} \sigma^{\nu]\alpha} \gamma_5 \Delta_\alpha}{2m_N^2} \widetilde{A}_{T1}^q(t) \Big\} u(p, S)\,,\end{aligned} \tag{4}$$

[a] Note that the parton distributions are boost independent. However, the variable $x$ maps into the momentum fraction of quarks and gluons only in the formalism of light-cone quantization, which is equivalent to Feynman's parton model in the infinite momentum frame $p_z \to \infty$. In the rest frame of the nucleon, for example, $x$ is just a special combination of the parton's off-shell energy $k_0$ and momentum $k_z$.

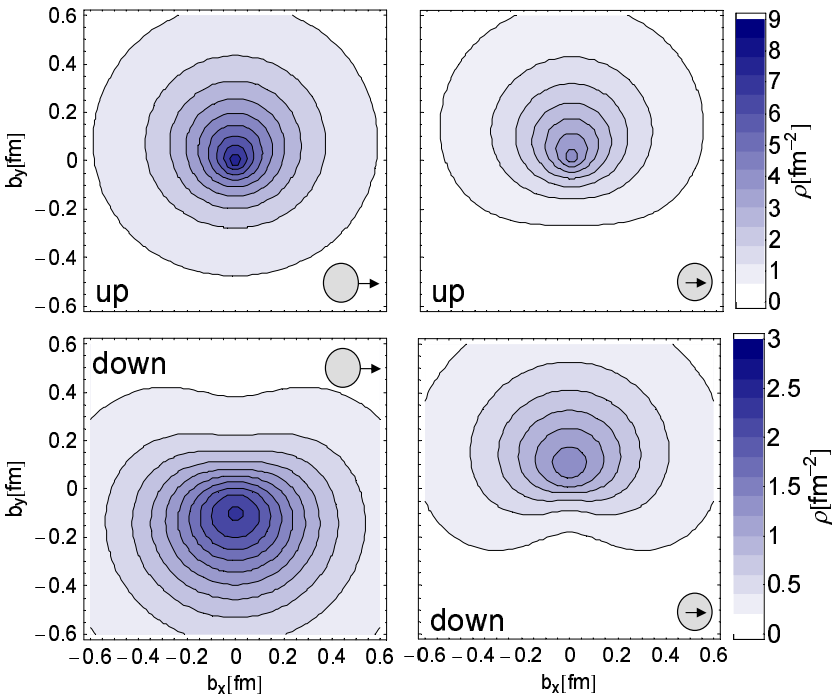


Figure 2. The first moment $\rho^{q\,1}(b_\perp, s_\perp, S_\perp)$ for unpolarized quarks in the transversely polarized proton (left panels) and transversely polarized quarks in the unpolarized nucleon (right panels) separately for up (top panels) and down (bottom panels) quarks. The direction of the quark (nucleon) spin is indicated by the inner (outer) arrows.

where $\mathcal{O}_T^{q\,\mu\nu} = \bar{q}\sigma^{\mu\nu}\gamma_5 q$ is the lowest operator of a tower of quark helicity flip operators, and $t = (p' - p)^2$. The impact parameter space GFFs that enter in (3) are obtained by Fourier transform

$$X(b_\perp^2) = \int \frac{d^2\Delta_\perp}{(2\pi)^2} \mathrm{e}^{-ib_\perp \Delta_\perp} X(t = -\Delta_\perp^2)\,, \tag{5}$$

where $\Delta_\perp$ is the transverse momentum transfer to the nucleon.

The calculations are done on gauge field configurations with $N_f = 2$ flavours of light dynamical sea quarks. The calculation proceeds in four steps. In the first step we compute the GFFs on any of our lattices, which differ essentially by the quark mass and the lattice spacing $a$. In the second step we fit the lattice data to a suitable parameterization. It turns out that the data can be well described by a $p$-pole ansatz $X(t) = X(0)/(1 - t/(pm_X^2))^p$. In the third step we extrapolate the results to the physical quark mass. To do so, we make use of the predictions of chiral perturbation theory (ChPT) as far as possible. The interested reader will find a more detailed discussion of the general procedure in the literature[5–7]. Finally we Fourier transform the GFFs to impact parameter space. We do not see any significant dependence on the lattice spacing $a$ in the range of lattice spacings $0.07 \lesssim a \lesssim 0.1$ fm we have explored, indicating that cut-off effects are small. The

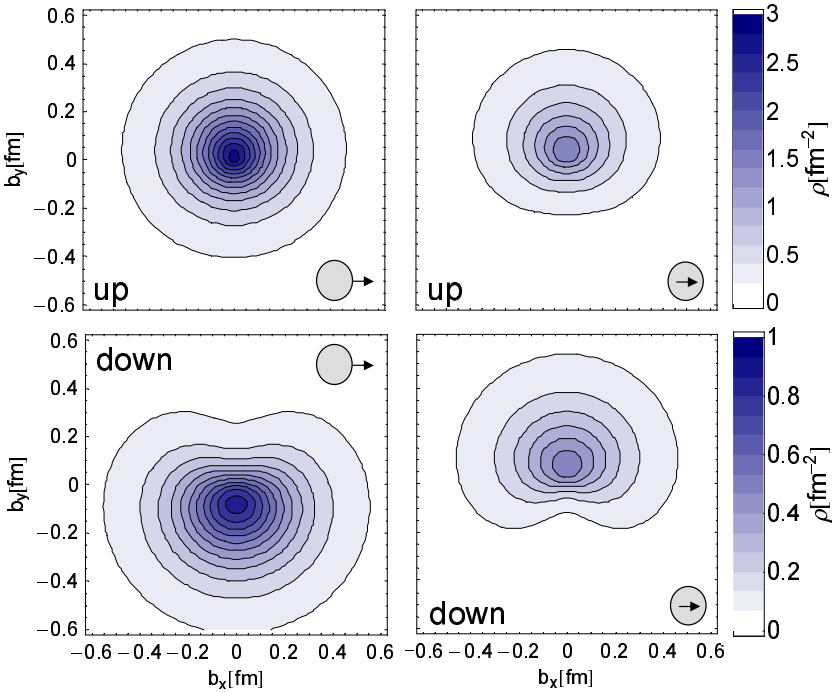


Figure 3. The second moment $\rho^{q\,2}(b_\perp, s_\perp, S_\perp)$. The notation and arrangement is the same as in Fig. 2.

hadronic matrix elements that enter the calculation of the GFFs need to be renormalized, which is done nonperturbatively[8].

In Fig. 2 we show the first moment $\rho^{q\,1}(b_\perp, s_\perp, S_\perp)$ separately for up and down quarks in the proton. We find strong distortions of unpolarized quarks in the transversely polarized proton (left panels), with the up and down quarks shifted in opposite direction. This distortion can be explained by orbital motion of the quarks[9], assuming that the orbital angular momentum $L_q$ of the up (down) quark is negative (positive). Recent lattice calculations have shown that this is indeed the case. Note that there is no gluon transversity, which could mix with quarks under evolution. As a result, the transverse spin structure is essentially valence-like, and we expect that the transverse spin and transverse orbital angular momentum are simply aligned. For transversely polarized quarks in the unpolarized proton (right panels) the densities for up and down quarks are both shifted in the positive $y$-direction. This is due to rather large and positive values of the tensor GFFs $\overline{B}^u_{Tn}(t=0)$ and $\overline{B}^d_{Tn}(t=0)$. In Fig. 3 we show the second moment $\rho^{q\,2}(b_\perp, s_\perp, S_\perp)$. The pattern is very similar to that in Fig. 2. The main difference is that the spin densities are more peaked towards $b_\perp = 0$.

Further information about the spin structure of the nucleon is obtained from considering transversely polarized quarks in the transversely polarized nucleon. In Fig. 4 we plot the first moment $\rho^{q\,1}(b_\perp, s_\perp, S_\perp)$ for $S_\perp$ and $s_\perp$ being (anti-)parallel resp. orthogonal to each other. A rich pattern of distortions is observed.

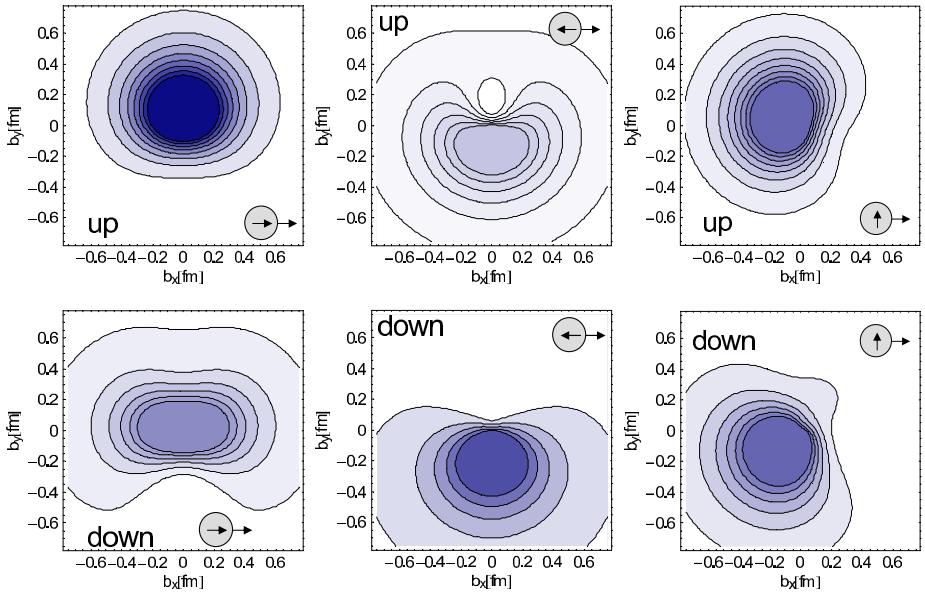


Figure 4. The first moment $\rho^{q\,1}(b_\perp, s_\perp, S_\perp)$ for nucleon and quarks both being polarized. The notation is the same as in Fig. 2.

## 3 Spin Structure of the Pion

Let us now turn to the pion[10]. As the pion has no spin, the impact parameter GPDs are much simpler than in the case of the nucleon. While the longitudinal spin structure of the pion is trivial, nothing is known about the transverse spin distribution. In this case the spin density reduces to

$$\rho^{q\,n}(b_\perp, s_\perp) = \int_{-1}^{1} dx\, x^{n-1} \rho^q(x, b_\perp, s_\perp) = \frac{1}{2}\Big\{ A_n^q(b_\perp^2) - \frac{b_\perp^j \epsilon^{ji} s_\perp^i}{m_\pi} B_{Tn}^{q\,\prime}(b_\perp^2) \Big\}\,, \quad (6)$$

and the GFFs $B_{Tn}^q$ are obtained from off-forward pion matrix elements of the form

$$\langle p' |\, \mathcal{O}_T^{q\,\mu\nu} \,| p \rangle = \frac{\bar{p}^\mu \Delta^\nu - \Delta^\mu \bar{p}^\nu}{m_\pi}\, B_{T1}^q(t)\,, \quad (7)$$

where $\bar{p} = (p' + p)/2$.

In Fig. 5 we plot the first two moments of $\rho^q(x, b_\perp, s_\perp)$. Like in the nucleon, the transversely polarized quarks are substantially distorted, which reveals, for the first time, a nontrivial spin structure of the pion.

The fact, that the distortion in both the pion and nucleon is of the same sign and magnitude, suggests that $B_{Tn}^q(b_\perp^2)$ in the pion and $\overline{B}_{Tn}^q(b_\perp^2)$ in the nucleon are about equal. Both GFFs are directly related to the correlation between the quark's transverse spin and intrinsic transverse momentum through the Boer-Mulders function[11]. A possible explanation of this observation is that the quarks in the fast moving hadron are in an s-wave state with an admixture of p-wave by means of the lower Dirac component of the wave function[12].

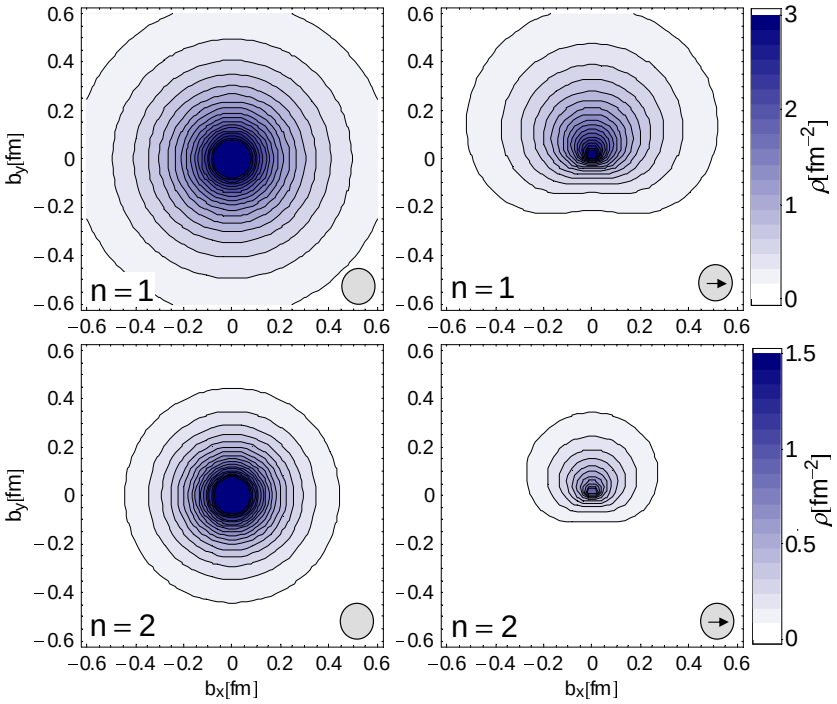


Figure 5. The first and second moment, $\rho^{q\,1}(b_\perp, s_\perp)$ and $\rho^{q\,2}(b_\perp, s_\perp)$, for unpolarized (left panels) and transversely polarized (right panels) up quarks in $\pi^+$.

As in case of the nucleon, we find that the second moment of $\rho^q(x, b_\perp, s_\perp)$ is more sharply peaked towards $b_\perp = 0$ than the first moment.

## 4 Conclusions

GPDs are a powerful tool in unravelling the microscopic structure of hadrons. We have seen that a profound understanding can be achieved through elaborate lattice simulations.

In the future we will need to extend our calculations to smaller quark masses and larger lattices to better constrain the parameterization of the GFFs as well as the extrapolation of the lattice results to the physical pion mass. We furthermore plan to extend the calculations to $N_f = 2 + 1$, and eventually $N_f = 2 + 1 + 1$, flavours of dynamical sea quarks.

## Acknowledgments

The simulations of the dynamical gauge field configurations have been performed on the BlueGene/L at KEK (Tsukuba), on the BlueGene/L at EPCC (Edinburgh) and on the BlueGene/L at NIC (Jülich). The analysis of the gauge field configurations has been done on the ape1000 and apeNEXT computers at DESY (Zeuthen). We thank all institutions for

their support. We furthermore acknowledge financial support by the Deutsche Forschungsgemeinschaft DFG through FOR-465 (Forschergruppe Gitter-Hadronen-Phänomenologie) and by the European Union through I3HP (Contract No. RII3-CT-2004-506078).

## References

1. M. Diehl, Phys. Rept. **388** (2003) 41 [hep-ph/0307382].
2. A. V. Belitsky and A. V. Radyushkin, Phys. Rept. **418** (2005) 1 [arXiv:hep-ph/0504030].
3. M. Göckeler, Ph. Hägler, R. Horsley, Y. Nakamura, D. Pleiter, P. E. L. Rakow, A. Schäfer, G. Schierholz, H. Stüben and J. M. Zanotti, Phys. Rev. Lett. **98** (2007) 222001 [arXiv:hep-lat/0612032].
4. M. Diehl and Ph. Hägler, Eur. Phys. J. C **44** (2005) 87 [hep-ph/0504175].
5. M. Göckeler, Ph. Hägler, R. Horsley, Y. Nakamura, M. Ohtani, D. Pleiter, P. E. .L. Rakow, A. Schäfer, G. Schierholz, W. Schroers, H. Stüben and J. M. Zanotti, arXiv:0709.3370 [hep-lat].
6. D. Brömmel, M. Göckeler, Ph. Hägler, R. Horsley, Y. Nakamura, M. Ohtani, D. Pleiter, P. E. .L. Rakow, A. Schäfer, G. Schierholz, W. Schroers, H. Stüben and J. M. Zanotti, arXiv:0710.1534 [hep-lat].
7. M. Göckeler, Ph. Hägler, R. Horsley, Y. Nakamura, M. Ohtani, D. Pleiter, P. E. .L. Rakow, A. Schäfer, G. Schierholz, W. Schroers, H. Stüben and J. M. Zanotti, arXiv:0710.2159 [hep-lat].
8. G. Martinelli, C. Pittori, C. T. Sachrajda, M. Testa and A. Vladikas, Nucl. Phys. B **445** (1995) 81 [hep-lat/9411010]; M. Göckeler, R. Horsley, H. Oelrich, H. Perlt, D. Petters, P. E. L. Rakow, A. Schäfer, G. Schierholz and A. Schillerg, Nucl. Phys. B **544** (1999) 699 [hep-lat/9807044].
9. M. Burkardt, Phys. Rev. D **66** (2002) 114005 [arXiv:hep-ph/0209179].
10. D. Brömmel, M. Diehl, M. Göckeler, Ph. Hägler, R. Horsley, Y. Nakamura, D. Pleiter, P. E. L. Rakow, A. Schäfer, G. Schierholz, H. Stüben and J. M. Zanotti, arXiv:0708.2249 [hep-lat].
11. D. Boer and P. J. Mulders, Phys. Rev. D **57** (1998) 5780 [arXiv:hep-ph/9711485].
12. M. Burkardt and B. Hannafious, arXiv:0705.1573 [hep-ph].